



<https://openaccess.leidenuniv.nl>

License: Article 25fa pilot End User Agreement

This publication is distributed under the terms of Article 25fa of the Dutch Copyright Act (Auteurswet) with explicit consent by the author. Dutch law entitles the maker of a short scientific work funded either wholly or partially by Dutch public funds to make that work publicly available for no consideration following a reasonable period of time after the work was first published, provided that clear reference is made to the source of the first publication of the work.

This publication is distributed under The Association of Universities in the Netherlands (VSNU) 'Article 25fa implementation' pilot project. In this pilot research outputs of researchers employed by Dutch Universities that comply with the legal requirements of Article 25fa of the Dutch Copyright Act are distributed online and free of cost or other barriers in institutional repositories. Research outputs are distributed six months after their first online publication in the original published version and with proper attribution to the source of the original publication.

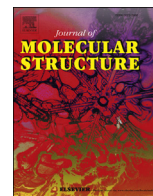
You are permitted to download and use the publication for personal purposes. All rights remain with the author(s) and/or copyrights owner(s) of this work. Any use of the publication other than authorised under this licence or copyright law is prohibited.

If you believe that digital publication of certain material infringes any of your rights or (privacy) interests, please let the Library know, stating your reasons. In case of a legitimate complaint, the Library will make the material inaccessible and/or remove it from the website. Please contact the Library through email: OpenAccess@library.leidenuniv.nl

Article details

Yu M., Every H.A., Jiskoot W., Witkamp G.-J. & Buijs W. (2018), Molecular structure of dextran sulphate sodium in aqueous environment, *Journal of Molecular Structure* 1156: 320-329.

Doi: 10.1016/j.molstruc.2017.11.090



Molecular structure of dextran sulphate sodium in aqueous environment

Miao Yu ^a, Hayley A. Every ^b, Wim Jiskoot ^c, Geert-Jan Witkamp ^a, Wim Buijs ^{d,*}

^a Department of Biotechnology, Delft University of Technology, Van der Maasweg 9, 2629, HZ, Delft, The Netherlands

^b FeyeCon Development & Implementation B.V., Rijnkade 17-A, 1382, GS, Weesp, The Netherlands

^c Division of Drug Delivery Technology, Cluster BioTherapeutics, Leiden Academic Centre for Drug Research (LACDR), Leiden University, Einsteinweg 55, 2333, CC, Leiden, The Netherlands

^d Department of Process & Energy, Delft University of Technology, Leeghwaterstraat 39, 2628, CB, Delft, The Netherlands

ARTICLE INFO

Article history:

Received 6 October 2017

Received in revised form

21 November 2017

Accepted 21 November 2017

Available online 23 November 2017

Keywords:

Molecular modelling

Molecular mechanics

α -1,6-D-glucose polymer

Helix

ABSTRACT

Here we propose a 3D-molecular structural model for dextran sulphate sodium (DSS) in a neutral aqueous environment based on the results of a molecular modelling study. The DSS structure is dominated by the stereochemistry of the 1,6-linked α -glucose units and the presence of two sulphate groups on each α -glucose unit. The structure of DSS can be best described as a helix with various patterns of di-sulphate substitution on the glucose rings. The presence of a side chain does not alter the 3D-structure of the linear main chain much, but affects the overall spatial dimension of the polymer. The simulated polymers have a diameter similar to or in some cases even larger than model α -hemolysin nano-pores for macromolecule transport in many biological processes, indicating a size-limited translocation through such pores. All results of the molecular modelling study are in line with previously reported experimental data. This study establishes the three-dimensional structure of DSS and summarizes the spatial dimension of the polymer, serving as the basis for a better understanding on the molecular level of DSS-involved electrostatic interaction processes with biological components like proteins and cell pores.

© 2017 Elsevier B.V. All rights reserved.

1. Introduction

Dextran sulphate sodium (DSS) is a polyanionic derivative of dextran with sodium sulphate groups ($-\text{OSO}_3\text{Na}$) attached to each repeating unit. DSS is widely applied in food, biotechnology, pharmaceutical and cosmetic industry and functions as coating material, anticoagulant agent, purification reagent, and conditioning agent [1–6]. DSS-involved interactions with protein materials have been widely studied with examples like DSS-protein complexation and particle formation for protein delivery purposes [7] and DSS passage through protein nano-channels inserted in a bilayer lipid membrane [8,9]. A realistic description of the three-dimensional (3D) structure of DSS and its flexibility is of utmost importance for a better understanding of the interaction between DSS and proteins, especially for the study relying on the spatial dimension of the polymer like the translocation via protein nano-channels.

* Corresponding author.

E-mail address: W.Buijs@tudelft.nl (W. Buijs).

Proposals for the 3D structure of polymeric carbohydrates have been mainly based on X-ray crystallography and nuclear magnetic resonance (NMR) measurements [10–13]. Whenever there is no experimental structure of a polymer available, especially in aqueous environment, and when it is extremely difficult to study the structure in a liquid environment in sufficient detail by experimental methods, molecular modelling can be an efficient tool to explore the structure. Molecular mechanics performs very well for a wide range of molecules throughout almost the entire periodic table. For large systems it is the only realistic option for molecular geometry optimization both with respect to accuracy of the structure and computational time. In this study, the Merck molecular force field (MMFF) [14,15] is used. The optimized geometries obtained by MMFF provide good starting structures for other studies like quantum mechanics modelling, molecular dynamics simulations, etc.

The molecular structures of monosaccharides, e.g., glucose, in aqueous environment have been widely studied by molecular modelling via molecular mechanics methods [16–19]. Geometric features like bond distances, bond angles, glucose ring conformation, and formation of hydrogen bridges with surrounding water

molecules were well elucidated. Oligosaccharides or polysaccharides, e.g., dextrans, have not been studied as much by molecular mechanics as monosaccharides [20,21]. Molecular modelling might shine light on characteristics like the rotation along glycosidic linkages and derived torsional angles, polymer elasticity, and competition among intramolecular hydrogen bridges and intermolecular hydrogen bridges. Up to now, literature reporting the molecular structure of sulphated polysaccharide derivatives is scarce [22], and as far as we know there are no publications presenting neither the experimentally nor the theoretically determined 3D-molecular structure of DSS. In this study, the 3D-structure of DSS is determined using an approach which can be applied to other (carbohydrate) polymers as well. The resulting DSS structure will be used to study the electrostatic interactions and structural dynamic behaviour with biological components like proteins and cell pores.

In this study, it is aimed to establish the molecular structure of DSS with an average molecular weight of 5000 Da, which value was chosen considering the frequent usage of this size of DSS. The parental polymer of DSS, dextran, is a highly-linear polymer of anhydroglucose produced by *Leuconostoc* spp. and related microorganisms, connected mainly via α -1,6-linkages. These α -D-glucans also possess side-chains, connected mainly via α -1,3- and occasionally via α -1,4- or α -1,2- branched linkages [23]. The exact structure of each type of dextran depends on its specific producing microbial strain and hence on the specific type of dextransucrase(s) involved [23,24]. Dextran, as the parental structure for the production of DSS, according to the manufacturer's information [25], is produced via an enzymatic process from *Leuconostoc mesenteroides*, strain B 512. The produced dextran contains 95% α -1,6-linkages and 5% α -1,3-branch linkages [26,27]. The sulfur content in DSS is about 17–18%, which is equivalent to approximately two $-\text{OSO}_3\text{Na}$ ester groups per glucose residue [28,29]. The $-\text{OSO}_3\text{Na}$ moieties can be located on different carbons of the glucose ring [30–33]. Carbon 2 and 3 (C-2,3) appear to be more reactive towards sulphation than the other carbon positions, and carbon 2, 3 and 4 (C-2,3,4) are the common sites for dextran di-sulphation [33,34]. C-2,3 are more suitable for di-substitution than carbon 2 and 4 (C-2,4) and carbon 3 and 4 (C-3,4) and all the three types of di-sulphation occur in the DSS product [30–34]. In our model, DSS structures with di-sulphation on C-2,3, C-2,4, and C-3,4 are used for structural determination.

2. Approach

An updated version of the Merck Molecular Force Field (MMFF), developed by Merck Research Laboratories [14], was applied. MMFF is an integral part of the Spartan'16 software package [15] which was used for all calculations.

A common DSS, obtained from Sigma Aldrich (Product Number: D7037), has an average molecular weight of 5000. This corresponds approximately to a dodecamer of α -1,6-D-glucose with two $-\text{OSO}_3\text{Na}$ moieties on each glucose ring. Although the material is delivered as a solid, it is commonly used in an aqueous solution. Therefore, particular attention was paid to the role of the aqueous solvent, not only in adding various amounts of H_2O explicitly, but also the building and construction of the $-\text{OSO}_3\text{Na}$ units on the sugar rings. They were introduced *in silico* as species in solution, which result in more accurate solvation energies in the molecular modelling calculations.

Starting from the established structure of α -D-glucose monomer, a tetramer was constructed with the correct stereochemistry around the 1,6-glycosidic bond [23–25]. A full conformer distribution (CD) of the tetramer was determined. From the obtained CD, low strain energy head-to-tail conformers were discarded, as these

showed intramolecular head-to-tail hydrogen bridges, which were considered unrealistic in aqueous environment. For the same reason, building a dodecamer of dextran based on dimeric or trimeric α -D-glucose was not a good approach. On the other hand, a real systematic search to a conformer distribution of the dodecamer generated a huge number of possible conformers, which would be too costly with respect to computational time. Thus, as an optimal feasible approach, the final conformation for the lowest-energy equilibrium conformer of the dodecamer of dextran was obtained by triplication of the best conformer of the tetramers, using the detailed geometric data of the connection between the second and the third glucose ring to construct the 4,5 and 8,9 couplings in the final dextran dodecamer. This was another strong reason to use the tetramer for building the dodecamer, as the tetramer is the smallest oligomer with 2 internal α -glucose units. Next, the final geometry of the dodecamer was obtained by an unrestricted normal geometry optimisation.

Two $-\text{OSO}_3\text{Na}$ groups in close vicinity on each α -D-glucose unit are the ionic functional groups on DSS. Regarding the fact that the ionic bonds between sodium cation and sulphate anion are subject to hydration, the optimised molecular structure of a sodium sulphate (Na_2SO_4) dimer in the presence of H_2O was studied before introducing these charged groups to the dextran dodecamer. The ionic option for the type of bonds between the sulphate anion and the sodium cation was chosen. Furthermore, explicit solvation with various numbers of H_2O was carried out.

On average, DSS contains two $-\text{OSO}_3\text{Na}$ ester groups per α -D-glucose unit. To study the effect of these strongly ionic groups on the structure of DSS, two $-\text{OSO}_3\text{Na}$ ester groups were added onto the positions C-2,3, C-2,4 and C-3,4 of the α -D-glucose unit. Next, CD's were determined for the three different α -D-glucose units with two $-\text{OSO}_3\text{Na}$ ester groups, while keeping the geometry of the sugar ring intact. Via these CD's, the preferred positions of the di- $-\text{OSO}_3\text{Na}$ ester groups as well as surrounding H_2O molecules to the α -D-glucose unit were obtained. In the later building process of the final DSS dodecamers, the preferred positions of the di- $-\text{OSO}_3\text{Na}$ ester groups and surrounding H_2O molecules were initially fixed in the model, followed by cutting them as a whole group. These fixed groups were connected to each α -D-glucose unit along the dextran dodecamer to achieve structures of DSS dodecamers containing 12 di- $-\text{OSO}_3\text{Na}$ ester groups and surrounding H_2O molecules. After completion of the building process, the connected di- $-\text{OSO}_3\text{Na}$ ester groups and surrounding H_2O molecules were unfixed, and an unrestricted full geometry optimization was carried out.

Statistically, there are about 5% of α -1,3 branched linkages among the DSS polymers. To study the influence of the side chain on the structure of DSS, a two-unit-long DSS moiety was connected to the DSS dodecamer with a α -C-1,3 linkage onto one of the α -D-glucose units, followed by geometry optimisation.

3. Results

3.1. 3D structure of dextran dodecamer

D-glucose, which is the monomeric unit of dextran, exists in two forms, α -D-glucose and β -D-glucose, which differ in the position of the hydroxyl ($-\text{OH}$) group on carbon 1 (C-1) of the glucose ring. The α -form has the OH group on C-1 on the opposite side of the methyl hydroxyl ($-\text{CH}_2\text{OH}$) group on carbon 6 (C-6). The β -form has both chemical groups on the same side. Fig. 1 shows the two forms with their strain energies from the MMFF calculation.

According to MMFF, α -D-glucose is slightly more stable than the β form, in line with previously reported theoretical and experimental results [35,36].

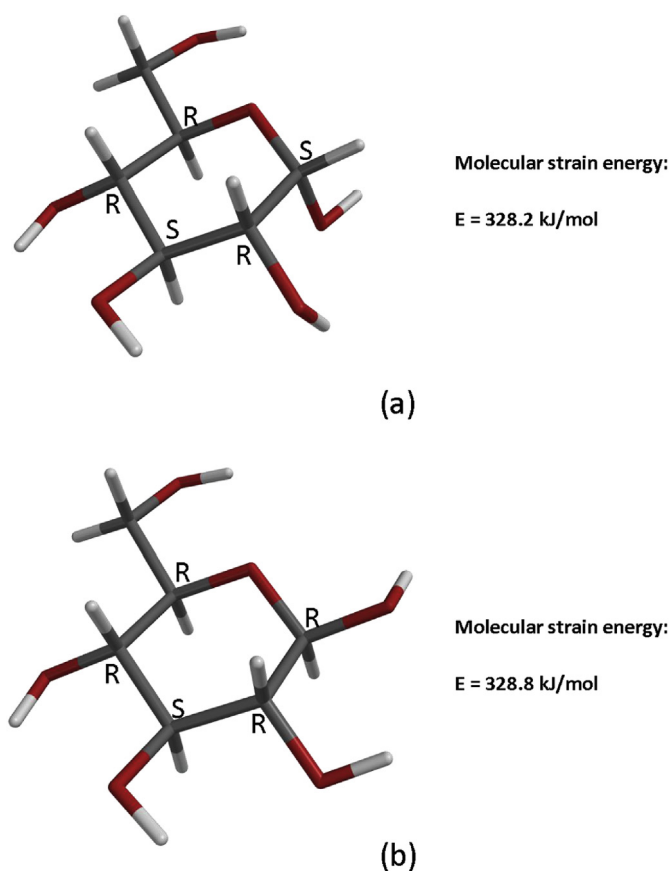


Fig. 1. Molecular structure displayed in a tube format of α -D-glucose (a) and β -D-glucose (b) and corresponding molecular strain energy. R and S indicate the absolute stereochemistry on the glucose carbons. Grey represents carbon, red oxygen and white hydrogen. This representation is applied in the following figures too.

The molecular structures of the α -D-glucose monomer, the α -D-dextran tetramer and the dodecamer are shown in Fig. 2. A helix structure was obtained for the dextran dodecamer. This structure served as the parental structure for the final DSS structures.

From the tetrameric structure presented in Fig. 2 (b), it can be seen that the first α -glucose ring shows a hydrogen bridge between the –OH group on carbon 6 (C-6) and the oxygen on C-5 in the ring, and the fourth glucose ring shows a hydrogen bridge between the –OH group on C-1 and the oxygen on C-2 of the third glucose ring. In constructing the final dodecamer of dextran, the geometry of the coupling between the second and the third α -glucose ring was taken, as this connection was not influenced by neither head nor tail interactions.

3.2. Equilibrium geometry of Na_2SO_4 dimer

Normally, dextran sulphates are supplied as sodium salts. In this study, we wanted to elucidate the structure of the dextran sulphate sodium (DSS) in neutral aqueous environment. As mentioned before, on average, two (– OSO_3Na) ester groups are located on one glucose ring in close vicinity. Therefore, the behaviour of two molecules of Na_2SO_4 in an aqueous environment was studied. Fig. 3 shows the equilibrium geometries of one and two Na_2SO_4 molecules with water as the solvent.

There is a strong interaction between sodium cations and sulphate anions. Three H_2O molecules strongly coordinate to sodium (charge: +1), and with a weaker H-bridge to sulphate-oxygen (charge: about –0.5). Together with the nearby sulphate-oxygen,

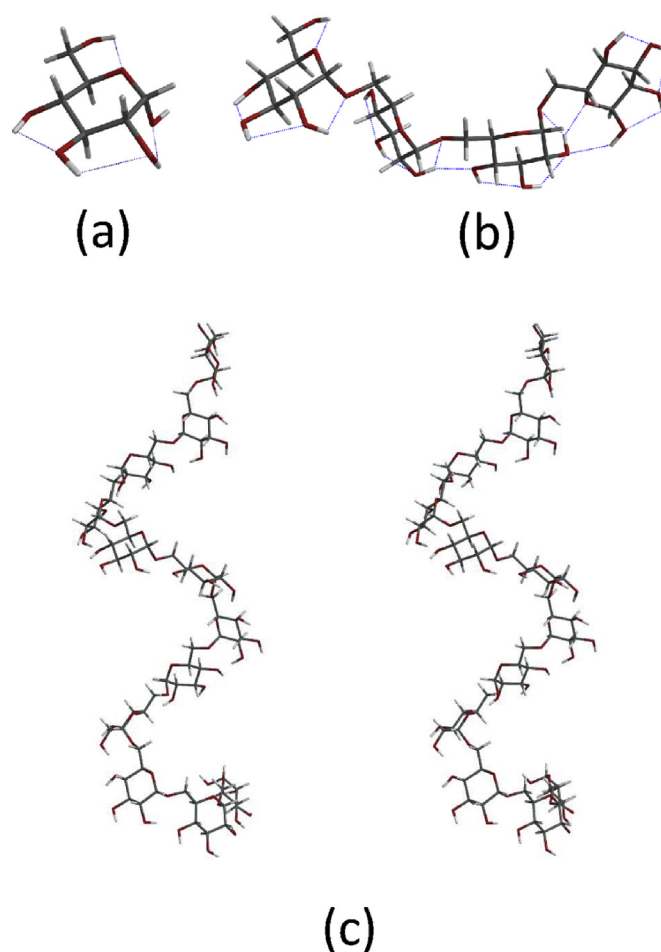


Fig. 2. MMFF-optimized equilibrium geometry of α -D-glucose monomer (a), tetramer (b) and dodecamer (c), where a cross-eyed stereo-pair picture of the dodecamer is displayed. The blue dashed lines represent hydrogen bridges. See Fig. 1 for explanation of the tube colors.

in total 5 oxygens coordinate to the Na cation. This is in line with previously reported studies on the hydration of the Na cation where 4–6 water-oxygen coordinate to one Na cation [37–39]. In the system of two Na_2SO_4 molecules, two Na cations are located in-between the two sulphates (Fig. 3 (b)). Now the above-mentioned 4–6 coordination of the Na cation is obtained with 2–3 sulphate-oxygens and 3 water-oxygens. Thus, three H_2O molecules close to one Na cation were used to describe the behavior of Na_2SO_4 in aqueous environment.

In DSS, the two Na cations will also be located in between the two sulphates which are held close together by their substitution pattern on the sugar ring.

3.3. Equilibrium geometry of DSS

There are documents stating that “DSS is produced via the esterification with sulphuric acid carried out under mild conditions” [25]. However, this cannot be the case as extensive depolymerization occurs under these conditions [40]. Therefore a powerful neutral sulphating agent like chlorosulphonic acid pyridine is mostly used to avoid polymer degradation [41,42]. Chlorosulphonic acid in pyridine was reported for the sulphation of dextran in previous studies [33,43].

Fig. 4 shows the monomeric α -D-glucose with different disulphation patterns optimized in MMFF with and without solvent

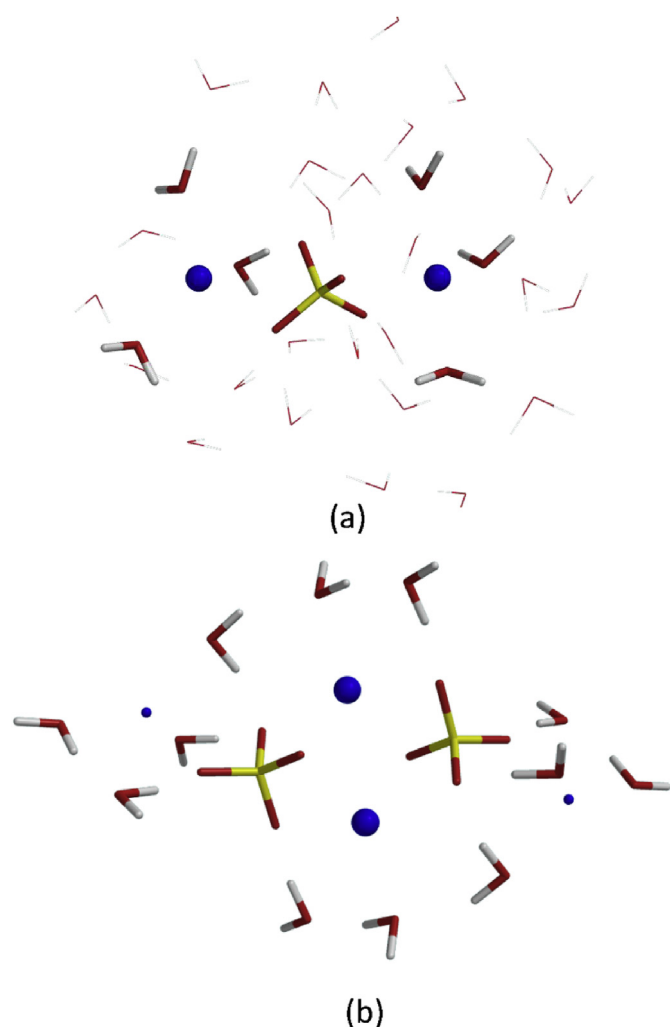


Fig. 3. (a): Equilibrium geometry of Na_2SO_4 in aqueous environment (with $32\text{H}_2\text{O}$ molecules); (b) two Na_2SO_4 molecules present with 12 surrounding (coordinating) H_2O molecules. In the figures, blue balls represent Na, S is in yellow and the thin wires represent H_2O . The two Na ions positioned in between the two sulphates are highlighted. All these representations are used for the following figures with corresponding formats.

water molecules. The sulphate groups are in equatorial position rather than axial position to avoid unfavorable sterical hindrance, similar to what was found before [34]. In addition, the two sulphate mono anions hold two Na cations in-between. In the di-sulphated glucose structure in the absence of H_2O , the sulphate-O to Na distance is about 2.1–2.2 Å and Na–Na distance is about 4.8 Å, while in the presence of H_2O , these values are about 2.1–4.1 Å and 5.2 Å respectively. These differences in atomic distances reflect the solvation power of H_2O . Thus, based on the studies above, combining the best conformer of the glucose with the best geometry of the two ($-\text{OSO}_3\text{Na}$) groups leads to the best structure for the monomeric di-sulphated glucose units. The latter were used to build the final DSS structures in the presence of H_2O .

Fig. 5 shows the DSS dodecamer structure in the presence of $72\text{H}_2\text{O}$ molecules, corresponding to $3\text{H}_2\text{O}$ per Na cation. The three DSS structures are helices, similar to that of the parental dextran structure. In each glucose unit, the two Na cations are located in-between the neighboring sulphate anions.

Table 1 shows the geometric properties of dextran dodecamer and DSS dodecamer under different conditions, including the dimensions and the average value of the pairs of dihedral angles,

which are illustrated in Fig. 6. The lengths of the various DSS dodecamers are about 40 Å. The length is measured as the distance between the tips of the helix ends. Uniformly substituted DSS dodecamers are longer than mixed substituted DSS dodecamers, however their diameters and band widths are approximately the average of the uniformly substituted DSS dodecamers. In order to get a quantitative impression of the effect of full aqueous solvation, the number of H_2O molecules in the mixed DSS dodecamer was increased to 1000 (see Fig. 7). The effect is a small increase in the geometric parameters of approximately 5%. Dextran shows energy minima at two dihedral angles of about 121 and 153° between each glucose ring, thus leading to 2^{11} possible conformers. As the energy difference between the two conformers is about 0.6 kJ/mol and the corresponding rotational barrier is about 11.6 kJ/mol only, the dextran helix structure will be very flexible with respect to these dihedrals.

Diameter and band width of DSS dodecamers (about 20 Å and 11 Å respectively) are larger than those of the dextran (about 16 Å and 9 Å respectively). The branched DSS obviously has a larger diameter (about 23 Å) than the linear DSS (about 20 Å).

Table 2 lists the results of the MMFF strain energies for C-2,3, C-2,4 and C-3,4 di-sulphated α -D-glucose monomers and the corresponding DSS dodecamers. They are in line with previously reported experimental results. It was stated that on the glucose ring, C-2 is the most active site for sulphation, followed by C-3 and then C-4. Thus after di-sulphation, the amount of C-2,3 di-sulphated species is higher than C-2,4 and C-3,4, which reflects the relative stability of the variously di-sulphated molecules [32,33].

3.4. Mixed type of di-sulphation

In reality DSS contains a mixture of various C-2,3, C-2,4 and C-3,4 di-sulphated polymers of different lengths, with an average chain length of 12. The average substitution pattern on the glucose rings is about C-2,3/C-2,4/C-3,4 = 6/5/1 in a random way [30–32]. The mixed structure shown in Fig. 7 is thus only one candidate out of thousands of structures with almost equal possibilities.

Comparing the geometric data of the mixed DSS dodecamer with uniform DSS dodecamer does not reveal large differences. Thus, the simulated DSS dodecamer can be considered as representative for real (mixed) DSS.

With 72 surrounding H_2O molecules (3 per sodium ion), the mixed DSS dodecamer shows a shrinkage compared with the uniform DSS (see Table 1). This is due to the closer interaction of $-\text{OSO}_3\text{Na}$ on adjacent glucose rings within the groove of the helix. The difference between the DSS structure with $72\text{H}_2\text{O}$ and $1000\text{H}_2\text{O}$ molecules is limited, as mentioned before.

3.5. DSS with side chain

Dextran is built up mainly based on α -(1,6) linkages (approximately 95%). The remaining 5% are α -(1,3) linkages account for the branching of dextran. The length of the side chains of dextran has been studied by sequential degradation and the results prove that more than 80% of the side chains contain less than 2 glucose units [23,44–48]. Fig. 8 shows the result of a structure with a side chain linked at the 6th unit of the DSS main chain via a 1,3 linkage. The side chain consisted of two units of 1,6-linked di-sulphated α -D-glucose. The helix of the main chain structure was preserved. Due to the presence of the side chain and its interaction with the main chain, the pitch of the helix was slightly shortened. Furthermore the orientation of the glucose planes as well as the attached ($-\text{OSO}_3\text{Na}$) groups were altered. Some $-\text{OSO}_3\text{Na}$ groups were positioned outwards, contributing to the increase of the measured length or diameter of the polymer geometry.

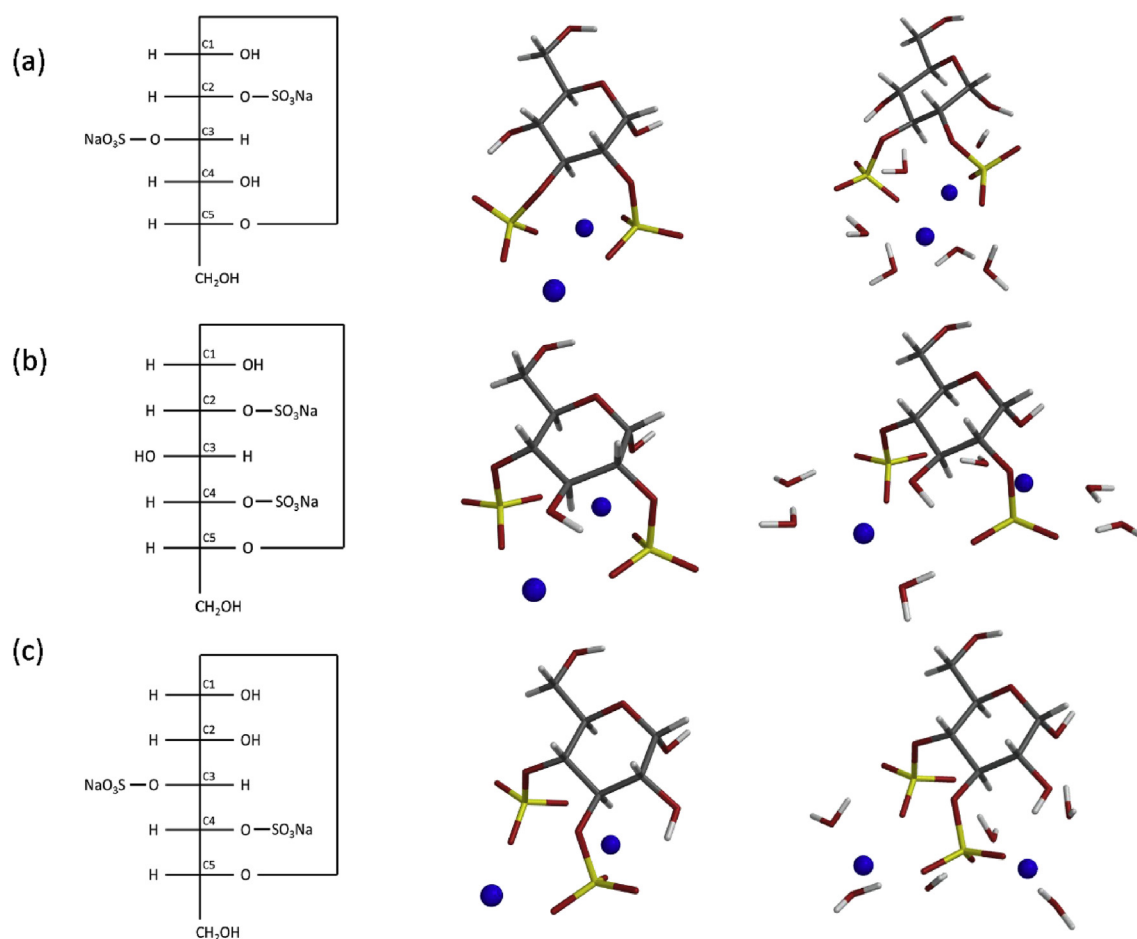


Fig. 4. The graphs in the left column represent the Fischer projection of di-sulphated monomeric glucose ring. The graphs in the middle are a translation of the Fischer projection images into 3D molecular structures. The graphs on the right show the di-sulphated monomeric glucose in the presence of H₂O. Row (a) represents a glucose with C-2,3 di-sulphation; (b) C-2,4 di-sulphation and (c) C-3,4 di-sulphation. See Fig. 1 and 3 for explanation of colors.

4. Discussion

4.1. Molecular structure of dextran

4.1.1. Enzymatic synthesis of dextran

Enzymatic synthesis of dextran was reported previously [49,50]. Dextranase catalyses the synthesis of dextran from sucrose. The proposed mechanism [23,51,52] is that dextran is biosynthesised by extrusion from the enzyme wherein glucose units are transferred from sucrose to the active site and inserted between the enzyme and the reducing end of the dextran polymer. The enzyme selectively makes an α -1,6 glycosidic bond between the glucose units during the extension of the dextran chain. The α -1,6 linkage between glucose rings is one of the common type of linkages in the molecule of dextran depending on the type of the producing microbial strain. The degree of polydispersity of dextran significantly affects its *in vivo* behaviour [53,54]. Native isolated dextran's are often polydisperse. The target chain length ranges from approximately 10 to 1000. Either partial acidic or enzymatic hydrolysis is applied to reduce the polydispersity of the dextran polymer and prepare the target size.

4.1.2. Conformation of six membered glucose ring and dextran

The structure of α -D-glucose has been described previously [16,55,56]. The glucose ring shows a normal chair conformation

with all -OH groups and the -CH₂OH group in an equatorial position, and only the glycosidic connection in an axial position due to the stereo selectivity of the enzyme.

Basic features determining polysaccharide structures, like dextran, have been described in Ref. [57]. The 3D structure of dextran is dominated by the α -(1,6) glycosidic linkage, which leads to two similar conformations with a different angle between the imaginary planes of the six membered rings of about 120 and 150° ($\Delta E \approx 0.6$ kJ/mol). Consequently, dextran adopts a slightly disordered helix structure [58]. The influence of thermal noise ($E \approx 2.4$ kJ/mol) on the rotation of the α -(1,6) glycosidic linkage is limited. Thus the dynamic randomness of dextran is limited to the two possible angles between the imaginary planes of the six membered rings. The optimised dextran dodecamer structure corresponds to one of the possible 2¹¹ very similar conformations of dextran present in natural aqueous environment.

4.1.3. Hydrogen bridges

The influence of hydrogen bridges is an important factor when dealing with modelling of carbohydrates and sugar-derived polymers in aqueous environment regarding the function of the maintenance of their preferred conformational structures. When simulating the carbohydrate in vacuum in the absence of H₂O, the conformation of the molecule tends to be dominated by energetically favorable intramolecular hydrogen bridges among hydroxyl-

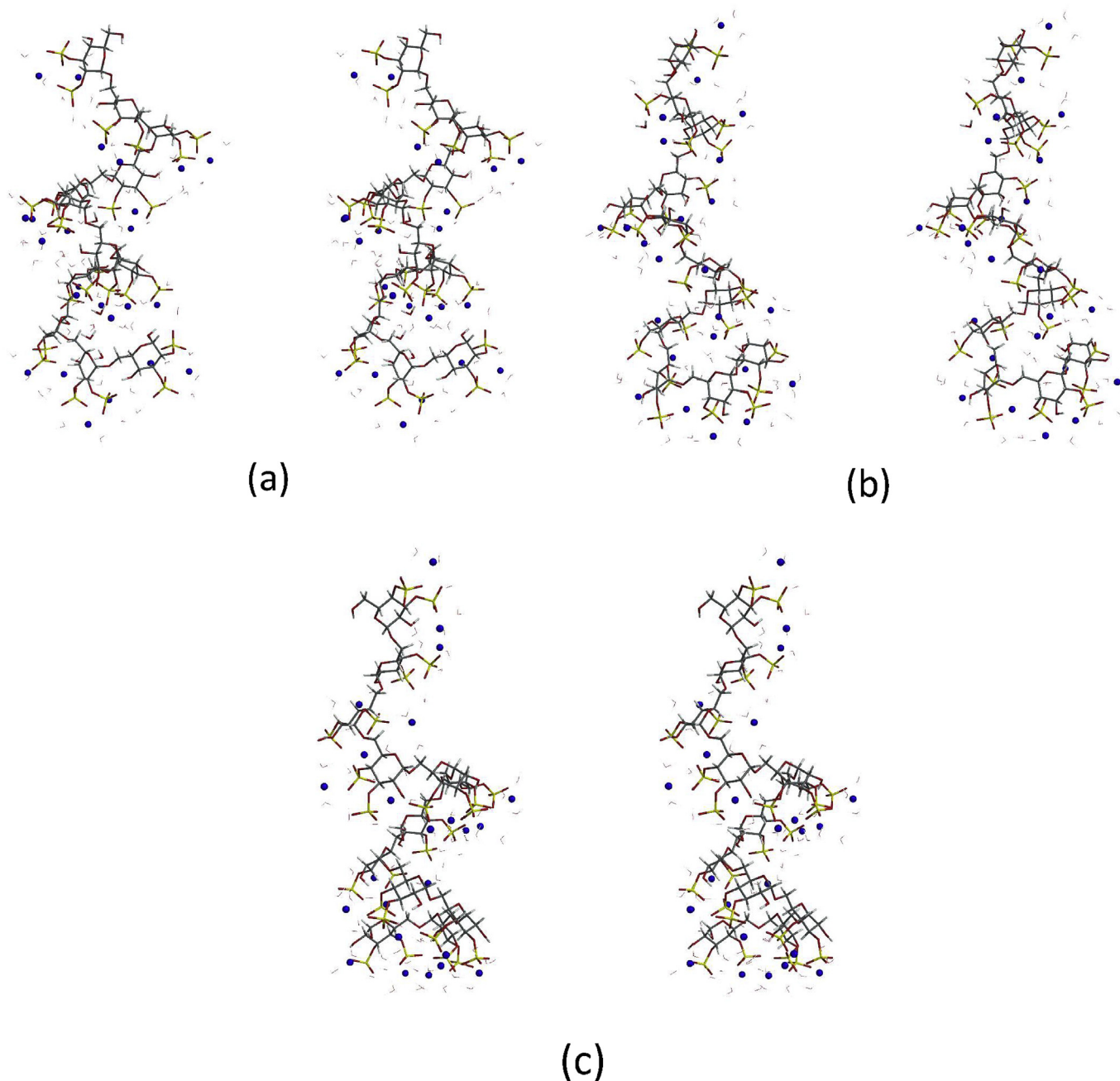


Fig. 5. Equilibrium geometries of C-2,3 (a), C-2,4 (b) and C-3,4 (c) DSS dodecamers with 72 surrounding H₂O molecules. Cross-eyed stereo-pair pictures are displayed. See Fig. 1 and 3 for explanation of colors.

hydrogen and neighboring oxygen with mostly a length of about 2.2–2.3 Å. These are weak hydrogen bridges with an energy of less than 17 kJ/mol [59]. However, in aqueous environment, the molecule tends to form hydrogen bridges with surrounding H₂O with 1.7–1.9 Å length, corresponding to a higher energy of about 17–60 kJ/mol [59]. In the presence of H₂O, intermolecular hydrogen bridges replace the intramolecular hydrogen bridges, but this formation of hydrogen bridges among the glucose moieties and surrounding H₂O does not cause any conformational change of the six membered ring [13].

4.1.4. Hydrogen bridges and $-\text{OSO}_3\text{Na}$ groups

The electrostatic functional groups ($-\text{OSO}_3\text{Na}$) along DSS were

proven to have no influence on the rotational dynamics of H₂O outside the first solvation shells of the ions, so no enhancement or breakdown of the hydrogen-bridge network in liquid water occurs [60]. In the DSS molecular structure worked out by modelling, there are two to three H₂O molecules located around each ionic group. The rest of the H₂O molecules, together with the hydrogen bridges among them, were little influenced by the presence of the polymer with ionized groups.

In conclusion no literature was found on the influence of hydrogen bridges on the structure of DSS, let alone the function of hydrogen bridges for relevant DSS-involved interaction with other biomolecular assemblies in aqueous environment.

Table 1
Characteristics of the helix conformation of dextran and DSS dodecamers.

Characteristics	DSS geometric properties in aqueous environment						
	Dextran	Types of di-sulphation ^a					
		C2,3	C2,4	C3,4	Mixed ^d	Mixed (1000H ₂ O)	Mixed (side chain) ^e
Dihedral angle ^{b,c}	120.5°; 153.4°	108.1°	129.1°	151.8°	126.8°	142.7°	–
Na to sulphate-O distance (Å)	–	2.5	3.0	3.1	2.7	3.3	–
Length (Å) ^c	43.9	41.5	42.1	42.9	39.0	41.1	41.6
Diameter (Å) ^c	16.2	20.3	18.7	19.5	19.8	20.7	22.6
Band width (Å) ^c	9.0	11.7	10.0	10.0	10.9	11.6	11.1

^a If not specified else, the DSS geometry is with 72H₂O molecules.

^b Average of dihedral angles along the DSS dodecamer structure.

^c See Fig. 6 for explanation of the various geometric properties.

^d Mixed: there is a statistical mixture of different di-sulphation patterns on the glucose rings of the dodecamer according to previously reported experimental results.

^e Mixed (side chain): attach a two units long side chain onto the linear DSS dodecamer.

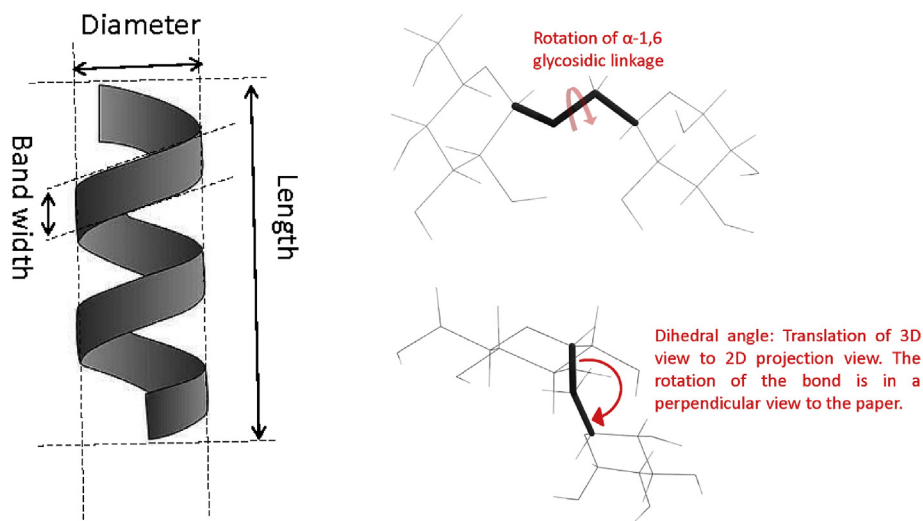


Fig. 6. Description of the geometric properties of the DSS helix molecule measured in this study and listed in Table 1.

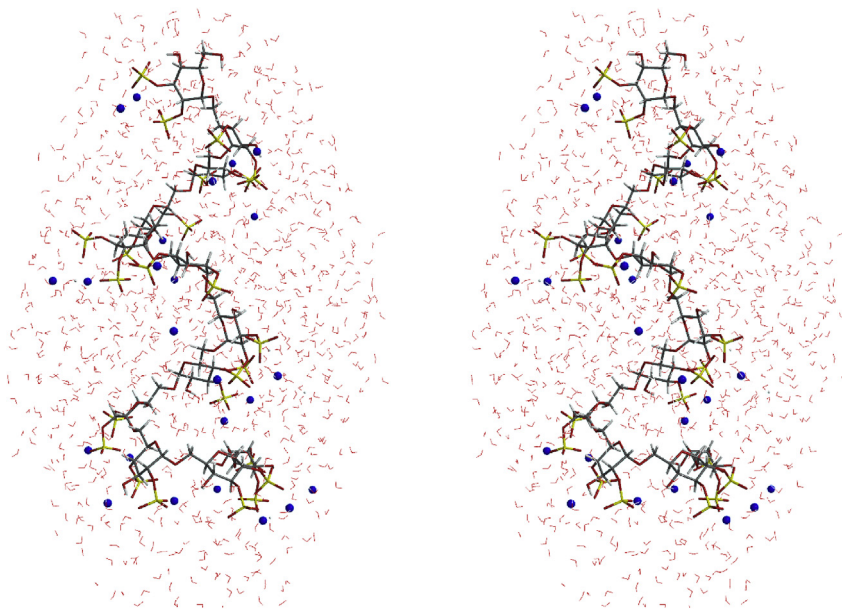


Fig. 7. Equilibrium geometry of DSS with quasi randomly-arranged mixed sulphation in the presence of 1000 water molecules. In detail, C-2,3 di-sulphation for glucose units 1, 3, 5, 7, 9 and 11; C-2,4 di-sulphation for units 2, 4, 6, 10 and 12; C-3,4 di-sulphation for unit 8. A cross-eyed stereo-pair picture is displayed. See Fig. 1 and 3 for explanation of colors.

Table 2

Strain energy of di-sulphated glucose and DSS dodecamers with various types of di-sulphation calculated by MMFF.

Compound	Strain energy (kJ/mol)	
	Vacuum	Aqueous
α -D-glucose monomer 2,3-di-Na sulphate	-1433.0	-1854.4
α -D-glucose monomer 2,4-di-Na sulphate	-1419.9	-1840.3
α -D-glucose monomer 3,4-di-Na sulphate	-1393.4	-1802.3
α -1,6-D-dextran dodecamer 2,3-di-Na sulphate	-	-22178.3
α -1,6-D-dextran dodecamer 2,4-di-Na sulphate	-	-22022.5
α -1,6-D-dextran dodecamer 3,4-di-Na sulphate	-	-21954.5
α -1,6-D-dextran dodecamer mixed-type-di-Na sulphate	-	-21898.9

4.2. Molecular structure of DSS

4.2.1. Neutral sulphation procedure

Among the existing procedures of production of DSS, the best known procedure is the sulphation of polysaccharides with SO_3 -pyridine [61], *in situ* formed by chlorosulphonic acid pyridine. During the sulphation process, a neutral environment is maintained where the sulphate esterification takes place on the hydroxyl groups of dextran. After cation exchange from pyridinium to sodium, the final DSS is obtained. This sulphation procedure of dextran was shown not to distort the homogeneity of the dextran sample or the NMR spectrum of the poly-glucose structure, which indicates that no detectable degradation occurs in the process [33,62,63]. There is a preference of sulphation onto glucose regarding the activity of the $-\text{OH}$ groups on different carbons. At low sulphation degrees, the carbon atoms in the glucose ring have the reactivity $\text{C-3} > \text{C-2} > \text{C-4}$ towards sulphation, whereas at high degrees of sulphation, the order is $\text{C-3} \geq \text{C-2} > \text{C-4}$ [33].

4.2.2. The geometry of DSS and its polymerisation units

Similar to the explanation of the (dynamic) dextran structure, the structure of DSS is a dynamically-changing molecule with

flexibility in the rotational glycosidic linkage.

The introduction of $-\text{OSO}_3\text{Na}$ groups onto glucose rings along dextran influences the dimension of the polymer. Both diameter and band width of the polymer increase due to the bulky sulphate groups. However, the length of the polymer is little influenced with a difference of 1–3 Å.

A slight increase of size was observed with the addition of 1000 H_2O molecules compared to the DSS geometry with 72 surrounding H_2O molecules. This increase is a result of the formation of DSS- H_2O hydrogen bridges instead of intramolecular ones leading to a slight expansion of the polymer. In addition the distance between the Na cation and sulphate-oxygen also increases slightly.

In a previous study on molecules containing a Na cation and sulphate [64], it was found that the Na cation tends to form a bridge between sulphate groups through favorable interactions with the negatively charged oxygens. In the DSS case the two equatorial sulphate ester groups on each glucose ring keep the two corresponding Na cations together too.

The types of di-sulphation do not change the overall helical scheme of the molecule. This is in line with earlier reported findings that the molecular structure of heparin, another sulphated polysaccharide chain, is little affected by the varying substitutions and the presence of bulky, charged sulphate substituents [65].

4.3. Interactions of DSS with biological structures

4.3.1. Aspecific electrostatic interactions

DSS, as a widely applied polyanion, interacts with positively charged materials, like proteins, most likely in an aspecific way. One example may be the development of polyelectrolyte-encapsulated controlled drug delivery systems [66–68]. Whenever oppositely charged protein and polyelectrolyte are mixed, electrostatic absorption takes place and molecules tend to associate into nano- or micro-particles [7]. In this process, the charge properties of the interacting materials most likely dominate the interactions.

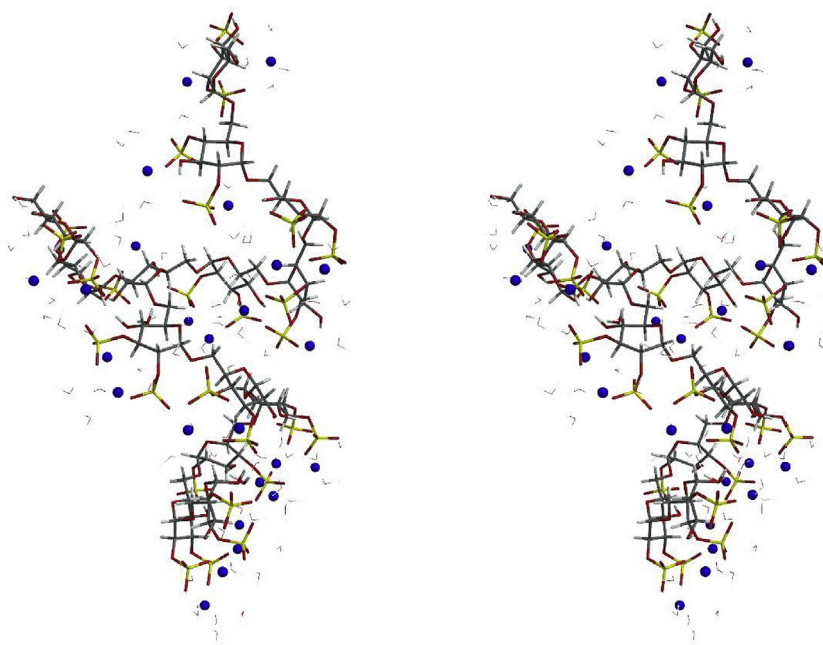


Fig. 8. DSS structure with a two units side chain connected via 1,3 linkages at the 6th unit of the mixed DSS dodecamer in the presence of 72 H_2O molecules. In detail, C-2,3 di-sulphation for glucose units 1,3,5,7,9 and 11; C-2,4 di-sulphation for units 2,4,10 and 12; C-3,4 di-sulphation for unit 8. A cross-eyed stereo-pair picture is displayed. See Fig. 1 and 3 for explanation of colors.

Table 3
DSS dimension according to MMFF modelling and reported dimensions of DSS and protein nano-pores in previous studies on polyelectrolyte translocation.

Reference	Size of DSS	Nanopore size	Comment
MMFF modelling	Mr. 5000 Da; length 4.1 nm; diameter 2.1 nm; band width 1.1 nm;	—	—
Teixeira et al. [70]	Mr. 5000–500,000 Da; Could enter the pore, but the entry of the entire molecule was precluded by branched structure.	Length \approx 10 nm; diameter \approx 2.6 nm.	α -hemolysin mesoscopic ion channel
Brun et al. [8]	Mr. 8000–500,000 Da; Diameter: 0.4 nm	—	An applied voltage-dependent transport was reported.
Pastoriza-Gallego et al. [69]	—	Pore diameter 1.4–4.6 nm.	α -hemolysin pore;
Gibrat et al. [71]	—	Pore diameter 2.0–2.6 nm.	α -hemolysin pore;

4.3.2. Specific size-dependent interaction with protein nano-pores

In some cases, specificity through size-dependent interactions can occur. Transport of macromolecules through membrane channels plays an important role in many biological processes and there have been studies dealing with the interactions of polyelectrolytes with protein nano-pores [69–71]. Besides the aspecific electrostatic interactions between charged groups or polymer complexation with local membrane functional groups, the topology of the interacting materials is a non-negligible factor, especially when the radius of the polymer is similar to the radius of the target pore. The present study indicates that the simulated DSS polymer has a diameter of about 1.9–2.2 Å, while some model α -hemolysin nano-pores have a size even smaller than the diameter of the DSS polymer (see Table 3) especially when there are side chains attached onto the polymer. The branched structure of DSS can preclude the entry of the entire molecule in the pore compared with linear polymers. The blockage by the polymer when entering the protein nano-pore is a dominating factor to be taken into account during polymer transport [8,72,73].

5. Conclusions

In this work, the 3D-geometry of the α -D-dextran dodecamer in aqueous environment was elucidated *in silico* based on the approach of careful expansion of the corresponding α -D-dextran monomer/tetramer units optimized by MMFF. The connections among the dextran units were based on the ones in the optimized tetramer without head-to-tail interactions. Two Na₂SO₄ moieties in aqueous environment were shown to be dimeric in nature, with 2–3 H₂O per Na cation as a sufficient hydration shell. The dimeric behavior was maintained in all glucose disulphates. DSS shows a helix structure, just like the parental dextran. The various helix structures of dextran and DSS originate from the two energy minima for the dihedral angle among adjacent sugar rings. The addition of two (–OSO₃Na) ester groups increases the diameter and band width of the polymer but has little influence on the polymer length. In the presence of 1000 surrounding H₂O molecules, a slight expansion of the polymer occurs. Still the Na cations tend to be positioned between the two (–OSO₃Na) ester groups on each glucose unit. The interaction of DSS involved in an encapsulating process is mainly aspecific, and just based on electrostatic attraction among materials with opposite charge. However, size-dependent specific interactions dominate in processes like the interaction with the α -hemolysin nano-pores.

Acknowledgment

This work was supported by the Netherlands Organisation for Scientific Research Domain Applied and Engineering Sciences

(TTW) [project number 12144], which is partly funded by the Ministry of Economic Affairs.

Appendix A. Supplementary data

Supplementary data related to this article can be found at <https://doi.org/10.1016/j.molstruc.2017.11.090>.

References

- [1] S. Samant, R. Singhal, P. Kulkarni, D. Rege, *Int. J. food Sci. Technol.* 28 (1993) 547–562.
- [2] N.G. Balabushevich, O.P. Tiourina, D.V. Volodkin, N.I. Larionova, G.B. Sukhorukov, *Biomacromolecules* 4 (2003) 1191–1197.
- [3] C. Schmitt, C. Sanchez, S. Desobry-Banon, J. Hardy, *Crit. Rev. Food Sci. Nutr.* 38 (1998) 689–753.
- [4] M. Miyake, Y. Kakizawa, *J. Cosmet. Sci.* 61 (2010) 289.
- [5] R. Yamagishi, M. Niwa, S.i. Kondo, N. Sakuragawa, T. Koide, *Thrombosis Res.* 36 (1984) 633–642.
- [6] M. Hall, C. Ricketts, *J. Clin. pathology* 5 (1952), 366–366.
- [7] A.S. Sediq, M.R. Nejadnik, I. El Bialy, G.J. Witkamp, W. Jiskoot, *Eur. J. Pharm. Biopharm.* 93 (2015) 339–345.
- [8] L. Brun, M. Pastoriza-Gallego, G. Oukhaled, J. Mathe, L. Bacri, L. Auvray, *J. Pelta, Phys. Rev. Lett.* 100 (2008), 158302.
- [9] G. Oukhaled, L. Bacri, J. Mathe, J. Pelta, L. Auvray, *EPL Europhys. Lett.* 82 (2008) 48003.
- [10] B. Mulloy, *An. Acad. Bras. Ciencias* 77 (2005) 651–664.
- [11] B. Mulloy, M. Forster, C. Jones, D. Davies, *Biochem. J.* 293 (1993) 849–858.
- [12] J. Lando, H. Olf, A. Peterlin, *J. Polym. Sci. Part A-1 Polym. Chem.* 4 (1966) 941–951.
- [13] P. Carçabal, R.A. Jockusch, I. Hünig, L.C. Snoek, R.T. Kroemer, B.G. Davis, D.P. Gamblin, I. Compagnon, J. Oomens, J.P. Simons, *J. Am. Chem. Soc.* 127 (2005) 11414–11425.
- [14] T.A. Halgren, *J. Comput. Chem.* 17 (1996) 490–519.
- [15] Spartan '16 is a product of Wavefunction, Inc., 18401 Von Karman Avenue, Suite 370, Irvine, CA 92612 U.S.A. (<http://www.wavefun.com>).
- [16] G. Jeffrey, R. Taylor, *J. Comput. Chem.* 1 (1980) 99–109.
- [17] L. Kroon-Batenburg, J. Kanter, *Acta Crystallogr. Sect. B Struct. Sci.* 39 (1983) 749–754.
- [18] S.E. Barrows, J.W. Storer, C.J. Cramer, A.D. French, D.G. Truhlar, *J. Comput. Chem.* 19 (1998) 1111–1129.
- [19] S. Pérez, M. Kouwijzer, K. Mazeau, S.B. Engelsens, *J. Mol. Graph.* 14 (1996) 307–321.
- [20] A.D. French, M.K. Dowd, *J. Mol. Struct. THEOCHEM* 286 (1993) 183–201.
- [21] B.A. Burton, D.A. Brant, *Biopolymers* 22 (1983) 1769–1792.
- [22] B. Mulloy, M.J. Forster, *Glycobiology* 10 (2000) 1147–1156.
- [23] M. Naessens, A. Cerdobbel, W. Soetaert, E.J. Vandamme, *J. Chem. Technol. Biotechnol.* 80 (2005) 845–860.
- [24] T.D. Leathers, *Biopolymers Online*, 2002.
- [25] M. Sigma Aldrich, USA, in.
- [26] N.W. Cheetham, E. Fiala-Beer, G.J. Walker, *Carbohydr. Polym.* 14 (1990) 149–158.
- [27] I. Sims, A. Thomson, U. Hubl, N. Larsen, R. Furneaux, *Carbohydr. Polym.* 45 (2001) 285–292.
- [28] J.C. Salamone, *Polymeric Materials Encyclopedia*, Twelve Volume Set, Taylor & Francis, 1996.
- [29] E.A. Balazs, R.W. Jeanloz, *Metabolism and Interactions: the Chemistry and Biology of Compounds Containing Amino Sugars*, Academic Press, 2013.
- [30] K.G. Ludwig-Baxter, R.N. Rej, A.S. Perlin, G.A. Neville, *J. Pharm. Sci.* 80 (1991) 655–660.
- [31] G.A. Neville, P. Rochon, R.N. Rej, A.S. Perlin, *J. Pharm. Sci.* 80 (1991) 239–244.
- [32] H. Miyaji, A. MISAKI, *J. Biochem.* 74 (1973) 1131–1139.

- [33] C. Mähner, M.D. Lechner, E. Nordmeier, *Carbohydr. Res.* 331 (2001) 203–208.
- [34] M. Cakić, G. Nikolić, L. Ilić, S. Stanković, *Chem. Industry Chem. Eng. Q.* 11 (2005) 74–78.
- [35] W. Damm, in.
- [36] W.E. Mitch, T.A. Ikizler, *Handbook of Nutrition and the Kidney*, Lippincott William & Wilkins, Philadelphia, PA, 2010.
- [37] S.B. Rempe, L.R. Pratt, *Fluid Phase Equilibria* 183 (2001) 121–132.
- [38] J. Mähler, I. Persson, *Inorganic chemistry* 51 (2011) 425–438.
- [39] A.L. Van Geet, *J. Am. Chem. Soc.* 94 (1972) 5583–5587.
- [40] *Polysaccharides from Eukaryotes*, Wiley-VCH, Weinheim [u.a.], 2002.
- [41] M. Mauzac, J. Jozefonvicz, *Biomaterials* 5 (1984) 301–304.
- [42] F. Chaubet, J. Champion, O. Maïga, S. Mauray, J. Jozefonvicz, *Carbohydr. Polym.* 28 (1995) 145–152.
- [43] C. Ricketts, *Br. J. Pharmacol. Chemother.* 9 (1954) 224–228.
- [44] X. Zhang, J.-C. Wang, K.M. Lacki, A.I. Liapis, *J. Phys. Chem. B* 109 (2005) 21028–21039.
- [45] J.C. Rankin, A. Jeanes, *J. Am. Chem. Soc.* 76 (1954) 4435–4441.
- [46] R. Dimler, I. Wolff, J. Sloan, C. Rist, *J. Am. Chem. Soc.* 77 (1955) 6568–6573.
- [47] J. Van Cleve, W. Schaefer, C. Rist, *J. Am. Chem. Soc.* 78 (1956) 4435–4438.
- [48] O. Larm, B. Lindberg, S. Svensson, *Carbohydr. Res.* 20 (1971) 39–48.
- [49] H. Koepsell, H. Tsuchiya, *J. Bacteriol.* 63 (1952) 293.
- [50] E.J. Hehre, *J. Biol. Chem.* 163 (1946) 221–233.
- [51] J.F. Robytt, B.K. Kimble, T.F. Walseth, *Archives Biochem. biophysics* 165 (1974) 634–640.
- [52] V. Monchois, R.M. Willemot, P. Monsan, *FEMS Microbiol. Rev.* 23 (1999) 131–151.
- [53] E. Khalikova, P. Susi, T. Korpela, *Microbiol. Mol. Biol. Rev.* 69 (2005) 306–325.
- [54] R. Mehvar, *J. Control. release* 69 (2000) 1–25.
- [55] J.W. Brady, *J. Am. Chem. Soc.* 111 (1989) 5155–5165.
- [56] G.M. Brown, H.A. Levy, *Science* 147 (1965) 1038–1039.
- [57] D. Oakenfull, *Polysaccharide Association Structures in Food*, 1998, p. 15.
- [58] Y.H. Hui, *Handbook of Food Science, Technology, and Engineering-4 Volume Set*, CRC press, 2005.
- [59] G.A. Jeffrey, G.A. Jeffrey, *An Introduction to Hydrogen Bonding*, Oxford university press, New York, 1997.
- [60] A.W. Omta, M.F. Kropman, S. Woutersen, H.J. Bakker, *Science* 301 (2003) 347–349.
- [61] T. Bochkareva, B. Passet, K. Popov, N. Platonova, T. Koval'chuk, *Chem. Heterocycl. Compd.* 23 (1987) 1084–1089.
- [62] E. Novikova, V. Smychenko, A. Iozep, *Russ. J. Appl. Chem.* 80 (2007) 1151–1153.
- [63] D. Papy-Garcia, V. Barbier-Chassefière, V. Rouet, M.-E. Kerros, C. Klochendler, M.-C. Tournaire, D. Barritault, J.P. Caruelle, E. Petit, *Macromolecules* 38 (2005) 4647–4654.
- [64] C.D. Bruce, M.L. Berkowitz, L. Perera, M.D. Forbes, *J. Phys. Chem. B* 106 (2002) 3788–3793.
- [65] B. Mulloy, M.J. Forster, C. Jones, A.F. Drake, E.A. Johnson, D.B. Davies, *Carbohydr. Res.* 255 (1994) 1–26.
- [66] A.P. Johnston, C. Cortez, A.S. Angelatos, F. Caruso, *Curr. Opin. Colloid & Interface Sci.* 11 (2006) 203–209.
- [67] A. Verma, A. Verma, *Int. J. Pharm. Sci. Res.* 4 (2013) 1684.
- [68] S. Lankalapalli, V.M. Kolapalli, *Indian J. Pharm. Sci.* 71 (2009) 481.
- [69] M. Pastoriza-Gallego, G. Gibrat, B. Thiebot, J.M. Betton, J. Pelta, *Biochimica Biophysica Acta (BBA) - Biomembr.* 1788 (2009) 1377–1386.
- [70] L.R. Teixeira, P.G. Merzlyak, A. Valeva, O.V. Krasilnikov, *Biophysical J.* 97 (2009) 2894–2903.
- [71] G. Gibrat, M. Pastoriza-Gallego, B. Thiebot, M.-F. Breton, L. Auvray, J. Pelta, *J. Phys. Chem. B* 112 (2008) 14687–14691.
- [72] J.B. Heng, C. Ho, T. Kim, R. Timp, A. Aksimentiev, Y.V. Grinkova, S. Sligar, K. Schulten, G. Timp, *Biophysical J.* 87 (2004) 2905–2911.
- [73] A. Aksimentiev, J.B. Heng, G. Timp, K. Schulten, *Biophysical J.* 87 (2004) 2086–2097.